Proceedings of the 9th U.S. National and 10th Canadian Conference on Earthquake Engineering
Compte Rendu de la 9ième Conférence Nationale Américaine et
10ième Conférence Canadienne de Génie Parasismique
July 25-29, 2010, Toronto, Ontario, Canada • Paper No

SEISMIC BEHAVIOR OF A HALF-THROUGH STEEL ARCH BRIDGE SUBJECTED TO GROUND MOTIONS AND FAULT DISPLACEMENT

T. Yamao[1], T. Sho[2], Y. Tsujino[2] and T. Mazda[1]

ABSTRACT

This paper presents the seismic behaviors of static pushover and dynamic response analyses of a half-through steel arch bridge subjected to earthquake waves and fault displacement. In static pushover analysis, the loading conditions were adjusted by controlling displacements at the end of stiffened girders and at the springings of arch ribs where the fault displacement was assumed to occur. In the dynamic response analyses, six seismic waves according to JSHB seismic waves were input and the seismic behaviors of the bridge model were discussed. Subsequently, both the 1999 Taiwan Ji-Ji Earthquake wave and the fault displacement wave obtained from the time integral of the acceleration response wave were applied and the response behaviors were investigated. The dynamic response analyses were carried out using earthquake waves including fault displacement in transverse, vertical and longitudinal (expanding and shrinking) directions in order to investigate seismic behaviors of the bridge model. According to the analytical results, it was found that the plastic members were clustered near the intersections of arch ribs and stiffened girders. The results of dynamic response analyses by the input of fault displacement show good agreement with those of the static analyses by displacement control method.

Introduction

When a strong earthquake occurs, steel arch bridges and steel bridge piers are frequently subjected to fault displacement induced by ground motion. Thus, it is still necessary to establish a method concerning the effect of fault displacement to check the seismic performance developed from nonlinear dynamic analysis for arch bridge design. Furthermore, it is needful to construct steel arch bridges possessing high seismic capacity at a minimum cost. Half-through type steel arch bridge is one of the arch bridges which reveals complicated behaviors when subjected to ground motion or ground displacement. However, seismic performance and failure behavior have not been yet clarified and only few studies concerning nonlinear seismic analysis when subjected to fault displacement have been reported (Japan Society of Civil Engineering

[1] Professor, Graduate School of Science and Technology, Kumamoto University, Kumamoto, Japan
[2] Engineer, Obayashi Corporation Co. Ltd., Tokyo, Japan

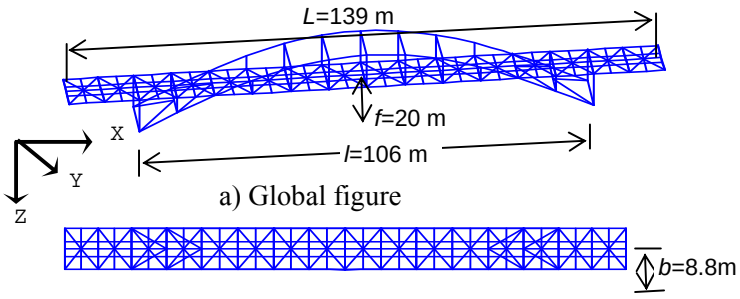

a) Global figure

b) Plane figure

Figure 1 Theoretical arch model

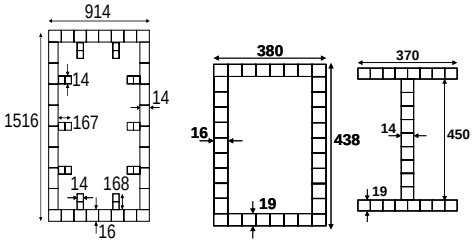

a) Arch rib b) Vertical column c) Lateral member

Figure 2 Cross sectional profiles of member

1999).

This paper presents the results of static pushover analysis and nonlinear dynamic response analysis of a half-through steel arch bridge subjected to earthquake waves including fault displacement in transverse, vertical and longitudinal (expanding and shrinking) directions. In static pushover analysis, the loading conditions were adjusted by controlling displacements at the end of stiffened girders and at the springings of arch ribs where the fault displacement was assumed to occur. In dynamic response analyses, the seismic behaviors of the bridge model subjected to Level II [JSHB, Japan Society of Civil Engineering (1999)] ground motion was discussed. Eventually, both the ground motion simulated from the 1999 Taiwan Ji-Ji Earthquake wave and the fault displacement wave obtained from the time integral of the acceleration response wave were input and compared with the results obtained from static pushover analysis.

Seismic Response Analysis

Theoretical Arch Model

The theoretical arch model studied herein is representative for actual deck-type arch bridges as shown in Figure 1.The Model, in which 11 vertical columns are hinged to arch ribs at both ends. The arch has a span length (l) of 106 m and the arch rise (f) is 20 m. The global axes of the arch ribs are also shown in Figure 1, where b and L represent the width of a stiffened girder and the deck span, respectively. The cross sectional profiles of vertical members and lateral members are rectangular and I-sections as shown in Figure 2(b) and 2(c). The model was assumed to have no residual stresses and initial crookedness modes. Material properties of the models used in the numerical analyses were assumed to be SM490Y steel type (JIS) with the yield stress (σ_y) of 353 MP_a and Young's modulus E was 206 GPa, respectively. Arch rise-to-span ratio (f/l) was taken to be 0.19 according to the condition of the actual arch bridges.

Numerical Analysis and the Input Seismic Waves

In static pushover analysis, the loading conditions were adjusted by controlling displacements at the end of stiffened girders and at the springings of arch ribs where the fault displacement was assumed to occur as shown in Figure 3. The 0.001m increment were applied until the displacement had reached 3.0 m in out-of-plane (transverse), in-plane (vertical) and longitudinal

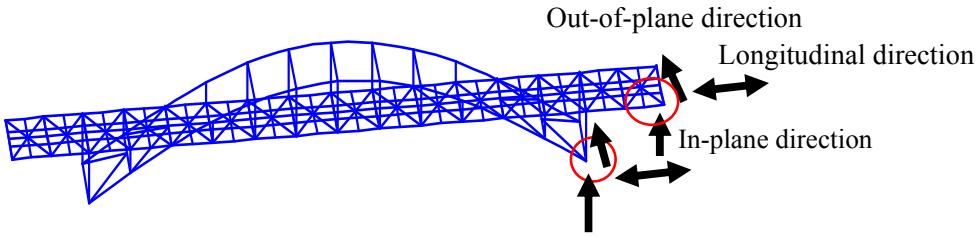

Figure 3 Loading conditions in static pushover analysis

directions, respectively. Six seismic waves (Type 1and Type 2) provided by the JSHB data and the 1999 Ji-Ji Earthquake wave [Japan Society of Civil Engineering (1999)] were input in the dynamic response analyses. The input JSHB seismic waves and the Ji-Ji earthquake wave are illustrated in Figure 4 and Figure 5. Type 2-I-1 and Type 2-I-2 waves were recorded at the Japan Metrological Agency (abbreviated by JMA) and the Japanese Railway Takatori Station (abbreviated by JRT) as the second level earthquake motion. Both waves are corresponding to the earthquake wave propagated under relatively soft ground condition and good diluvial ground conditions, respectively. The acceleration response spectrums of the Type 2-I-1 and Type 2-I-2 waves are shown in Figure 6 which the acceleration response spectrum of the E-W and N-S components of the JMA wave data.

For the 1999 Taiwan Ji-Ji Earthquake input wave, the relative large fault displacement measured after the earthquake was also concerned. Consequently, the fault displacement wave obtained from the time integral of the acceleration response wave was considered in the numerical analysis as indicated in Figure 5(b). Both the seismic waves illustrated in Figure 5(a) and the fault displacements TCU68EW2-5 and TCU68EW2-6 waves illustrated in Figure 5(b) were input in the dynamic response analyses. The maximum relative difference of two fault displacements is 1m. In order to simulate the movement at the arch springings, the TCU68EW2-5 wave was applied in longitudinal direction at the left arch sprnging and the TCU68EW2-6 wave was applied in longitudinal direction at the right arch sprnging, as mentioned in Figure 1(a), respectively.

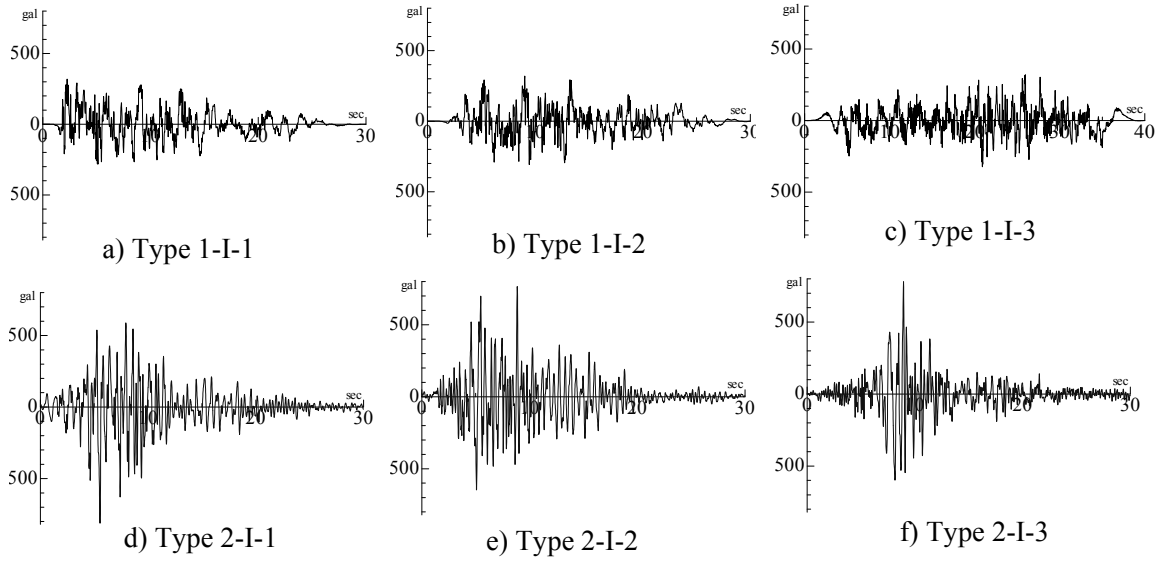

Figure 4 Input JSHB seismic waves

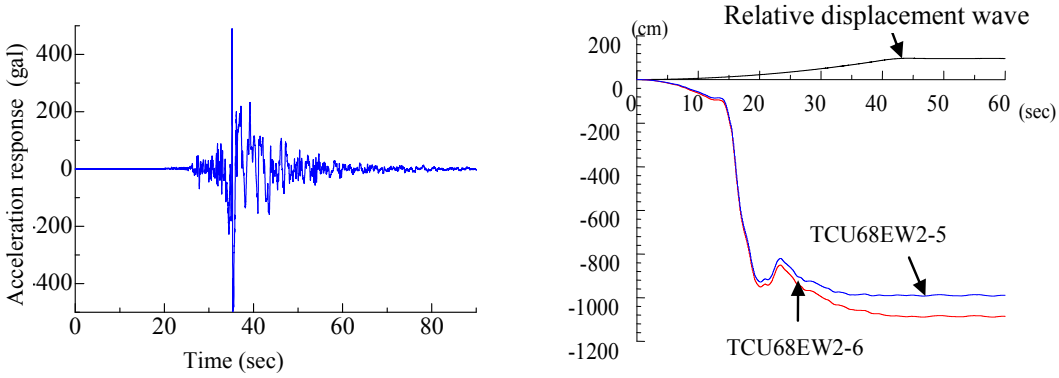

a) Input seismic wave b)Input fault displacement

Figure 5 1999 Ji-Ji Earthquake input wave

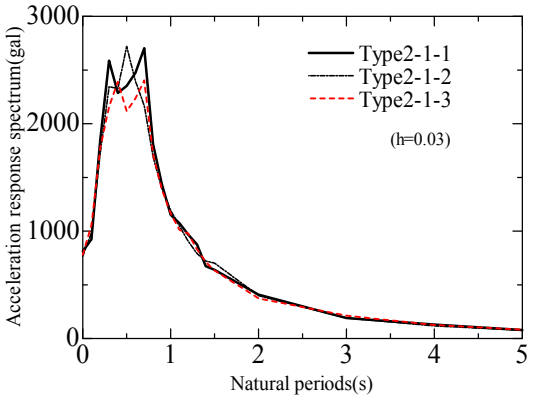

Figure 6 Acceleration response spectrum of Type 2 waves

Table 1 Results of eigenvalue analysis

Order of period	Natural frequency (Hz)	Natural periods (sec)	Effective mass ratio (%)		
			X	Y	Z
1	0.922	1.084	39	0	0
2	1.707	0.586	0	36	0
3	3.042	0.329	0	0	0
4	3.101	0.322	12	0	0
5	3.404	0.294	0	45	0
6	4.062	0.246	0	0	0
7	4.103	0.244	0	0	37
8	4.169	0.240	0	0	0
9	4.627	0.216	0	0	17
10	5.558	0.180	0	1	0

Eigenvalue Analysis

The eigenvalue analysis was carried out to investigate the effect of arch ribs and stiffened girders on the natural periods of the bridge model. In order to understand the fundamental dynamic characteristics, Table 1 presents the natural periods and the effective mass ratios of each predominant mode. The maximum effective mass ratios obtained in X, Y and Z directions imply the order of the dominant natural period. It can be seen from Table 1 that the arch bridge model is possible to vibrate sympathetically at the 9th mode since the dominant period is ranged between 0.2 - 0.3 sec.

Damping Matrix and Numerical Analysis

Numerical analyses were conducted using the Newmark-β method (β = 0.25) where the equations of motion were integrated with respect to time taking into account geometrical non-linearity. A constant time step of 0.001 sec and a damping model (Rayleigh type) calibrated to the initial stiffness and mass were utilized. The seismic response analysis with ground acceleration input and a constant dead load was performed using the nonlinear FEM program

TDAPIII, which is capable of taking into account geometric and material non-linearity. Six seismic waves were input in longitudinal (X-axis) direction and out-of-plane (Y-axis) direction, respectively.

Results and Discussions

Static Analysis by Displacement Control Method

Figure 7 shows the numbers of yielded elements of the arch model obtained by displacement control method in the longitudinal (expanding and shrinking), out-of-plane and in-plane directions. When 3.0 m displacement was applied in the longitudinal directions (expanding and shrinking), more than 40 elements were found yielded. However, no yielded element was found in in-plane direction. The results also indicate that the effect of the fault displacement direction on the damage of the arch bridge model is dominant. Figure 8 illustrates the deformation modes of the arch bridge in longitudinal direction (expanding and shrinking) when 3.0 m displacement was applied. The yielded elements corresponding to the deformation mode in Figure 8 is also illustrated in Figure 9. It can be seen that the plastic members are clustered beneath the joints of the arch ribs and stiffened girders. This is caused by the large deformation at this intersection zones as shown in Figure 8. Figure 10 shows the distribution of the maximum and the minimum plastic ratios of strain response of the arch rib and the stiffened girder in longitudinal directions. The strain ratio was plotted at 1.0m and 3.0m of displacement applied and non-dimensionalized parameter. The results coincide with the locations of yielded elements where the maximum strains of the arch rib occurred beneath the joints of the arch rib and the stiffened girder.

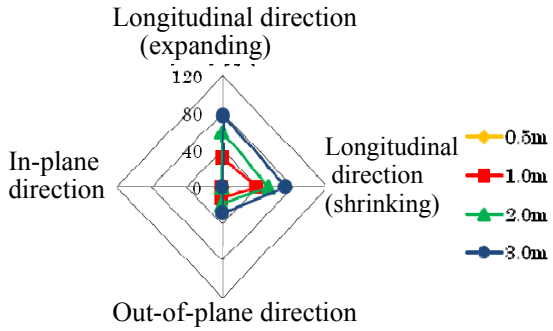

Figure 7 Numbers of yielded elements by displacement control method

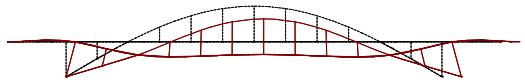

a) Longitudinal direction (expanding)

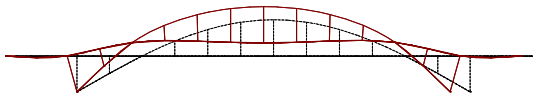

b) Longitudinal direction (shrinking)

Figure 8 Deformation modes of arch bridge in longitudinal direction

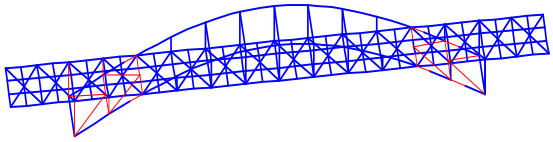

a) Longitudinal direction (Expanding)

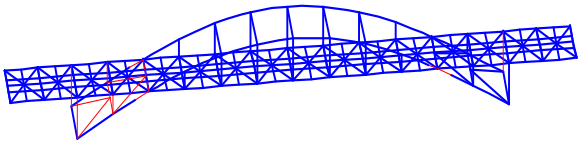

b) Out-of-plane direction

Figure 9 Distributions of plastic zones

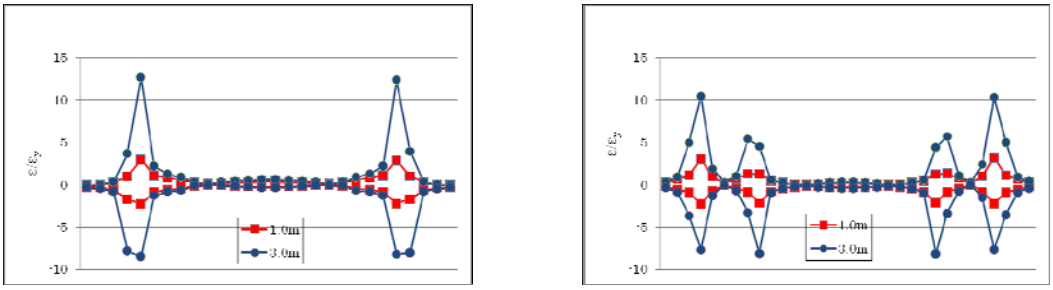

i) Longitudinal direction (expanding)

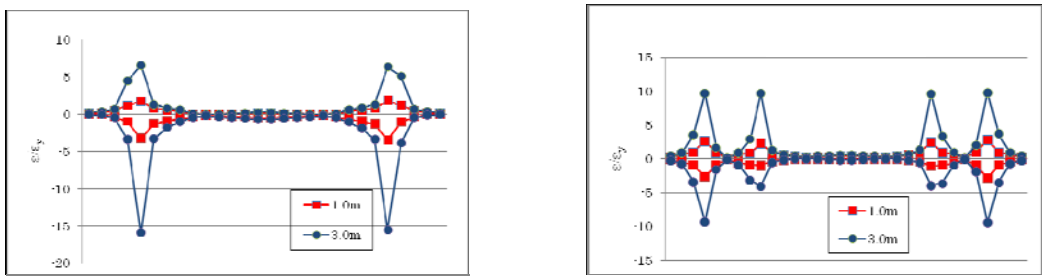

a) Arch rib

b) Stiffened girder

ii) Longitudinal direction (shrinking)

Figure 10 Distributions of maximum and minimum plastic ratios of strain

Seismic Response Behavior under Type 1 and Type 2 Ground Motions

Figure 11 shows the time-history data of displacement responses in longitudinal and out-of-plane directions at the arch crown when Type 2 ground motions were input. The vertical axis represents the displacement and the horizontal axis shows the elapsed time. The maximum and residual displacements in longitudinal and out-of-plane directions at the arch crown of the arch model under six seismic waves are indicated in Table 2. It can be seen that the maximum displace-ments taken from displacement responses in out-of-plane direction occurred under Type 2 ground motion. To understand the elasto-plastic behavior of the steel arch bridge in the longitudinal and out-of-plane directions, the stress-strain hysteresis curves of the members beneath the intersection of the arch rib and the stiffened girder at the most edge fiber elements where maximum values of stress and strain have been observed are demonstrated in Figure 12. The results indicate that both strain ratios developed in the arch rib and the stiffened girder are very small. Since the maximum strains in both the arch rib and the stiffened girder do not reach their yield strains, it can be judged that this half-through arch bridge model subjected to Level II ground motions is not damaged.

Table 2 Maximum and residual displacements at the arch crown

Type		1-I-1	1-I-2	1-I-3	2-I-1	2-I-2	2-I-3
Longitudinal direction (mm)	Maximum displacement	65.9	86.7	83.3	100.9	97.6	94.9
	Residual displacement	6.47	2.25	13.14	3.51	5.87	2.82
Out-of-plane direction (mm)	Maximum displacement	108.0	107.5	106.1	315.1	359.4	312.9
	Residual displacement	4.66	2.13	14.03	0.51	0.13	0.66

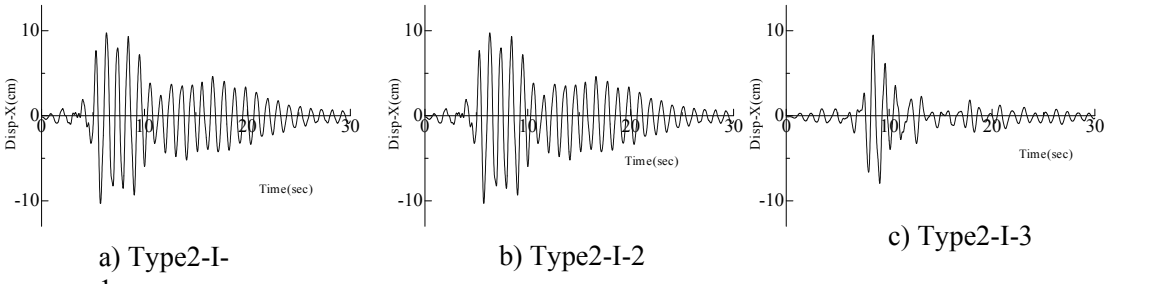

a) Type2-I-1 b) Type2-I-2 c) Type2-I-3

i) Longitudinal direction

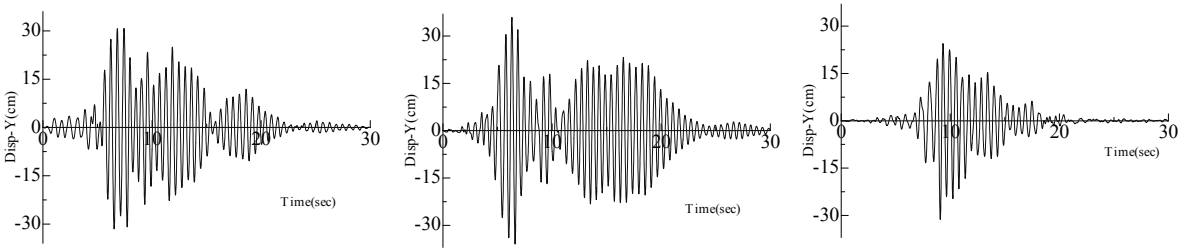

a) Type2-I-1 b) Type2-I-2 c) Type2-I-3

ii) Out-of-plane direction

Figure 11 Time-history data of displacement responses at the arch crown

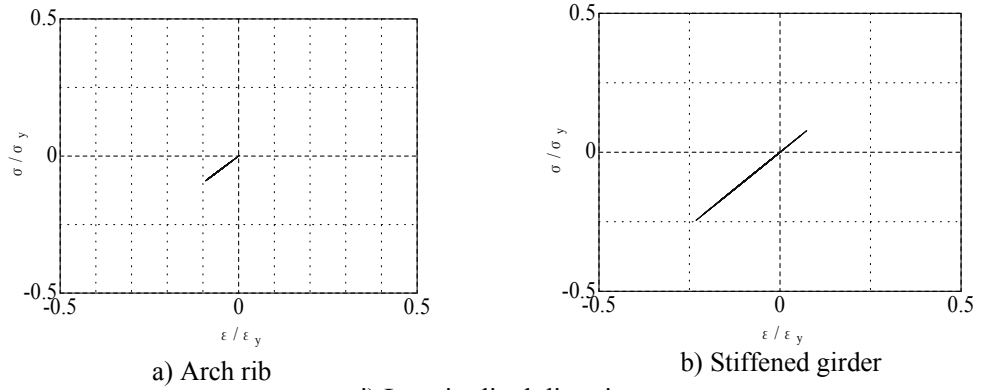

a) Arch rib b) Stiffened girder

i) Longitudinal direction

a) Arch rib b) Stiffened girder

ii) Out-of-plane direction

Figure 12 Stress-strain curves at the intersection of the arch rib and the stiffened girder

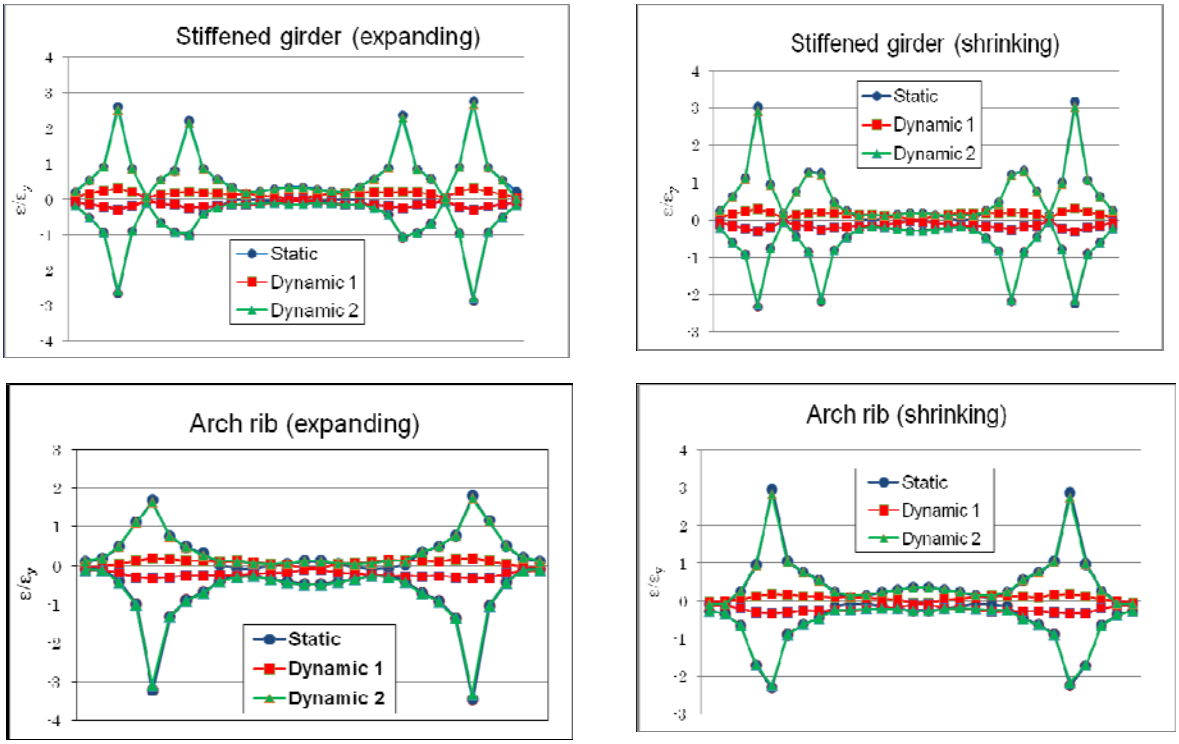

a) Longitudinal direction b) Longitudinal direction

Static: Static analysis by displacement control method (1.0 m)
Dynamic 1: Dynamic analysis using Ji-Ji Earthquake wave
Dynamic 2: Dynamic analysis by fault displacement obtained from Ji-Ji Earthquake

Figure 13 Comparisons of the maximum and minimum plastic ratios of strain response

Response Behavior of 1999 Ji-JI Earthquake Wave

Figure 13 shows the comparisons between the maximum and minimum plastic ratios $\varepsilon/\varepsilon_y$ of strain responses of the arch rib and the stiffened girder in longitudinal direction (expanding and shrinking). The results of the static analysis by displacement control method (1.0 m) was compared with the results of the dynamic analysis using Ji-Ji Earthquake wave and the dynamic response analyzed by the input of fault displacement (1.0 m) obtained from Ji-Ji Earthquake wave. From these figures, it was found that the maximum strains of the arch rib and the stiffened girder were clustered near the intersection of the arch rib and the stiffened girder. Furthermore, it is also recognized that the results of dynamic response analyses by the input of fault displacement (1.0 m) show good agreement with those of the static analyses by displacement control method corresponding to time which the strain ratios obtained.

Conclusions

Seismic behaviors of a half-through steel arch bridge subjected to ground motions and fault displacement in transverse, vertical and longitudinal directions were investigated by static pushover and dynamic response analyses. In nonlinear dynamic response analysis, six seismic waves according to JSHB seismic waves were simulated and discussed. Subsequently, both the

1999 Taiwan Ji-Ji Earthquake wave and the fault displacement wave obtained from the time integral of the acceleration response wave were input. The static pushover analysis by displacement control method was also carried out and compared. The conclusions of this study are summarized as the followings.

1) The effect of the fault displacement direction on the damage of the arch bridge model is dominant.
2) The Results obtained from both static and dynamic analyses indicate that the plastic members are clustered near the joints of the arch ribs and stiffened girders. This is caused by the large deformation at this intersection zones.
3) The maximum displacements taken from displacement responses in out-of-plane direction occur under Type 2 ground motion. However, the arch bridge model is not judged to damage because the maximum strains in members do not reach their yield strains.
4) The Results obtained from both static and dynamic analyses indicate that the maximum strains of the arch rib and the stiffened girder are clustered near the intersection of the arch rib and the stiffened girder.
5) The results of dynamic response analyses by the input of fault displacement (1m) show good agreement with those of the static analyses by displacement control method corresponding to time which the strain ratios obtained.

Acknowledgments

We wish to thank Mr. K. Yunoki, JIP Techno Science Co. Ltd. for his help and advice in carrying out this research.

References

Japan Society of Civil Engineering, 1999, The 1999 Ji-Ji Earthquake, Taiwan-Investigation into Damage to Civil Engineering Structure.

Japan Society of Civil Engineering , 1999, The 1999 Kocaeli Earthquake, Turkey-Investigation into Damage to Civil Engineering Structure.

Japan Road Association, 2002, *Specifications for Highway Bridges*, Part II Steel Bridge and Part V Seismic Design. (in Japanese)

NIPPON TDAPIII, 2005, *Ver2.13 User Manual*.

Yamao, T., Takaji T., and Atavit S. , 2006, Ultimate strength and behavior of deck-type arch bridges with curved pair ribs, *Proc. of Fourth International Conference on New Dimensions in Bridges, Flyovers & Elevated Structures*, Fuzhou, China, 317-324.

Yamao, T., Sho T., Murakami S. and Mazda T. , 2007, Seismic behavior and evaluation of seismic performance of half through steel arch bridges subjected to fault displacement, *Journal of Seismic Engineering ,* 317-324.